EXTREME ULTRAVIOLET HELIOGRAMS AND THE SUN'S CORONA *

J. D. Purcell, R. Tousey, and M. J. Koomen
E. O. Hulburt Center for Space Research
U. S. Naval Research Laboratory
Washington, D. C., 20390, U. S. A.

R-09-029-036

Presented

to

X COSPAR Assembly
London, U. K.

24 - 29 July 1967

* Supported, in part, by the National Aeronautics and Space Administration

7140-PRR-10/67:RT:MJK:mgw
July 1967

EXTREME ULTRAVIOLET HELIOGRAMS AND THE SUN'S CORONA*

J. D. Purcell, R. Tousey, and M. J. Koomen
E. O. Hulburt Center for Space Research
Naval Research Laboratory
Washington, D. C., 20390, U.S.A.

The extreme ultraviolet (XUV) spectroheliograms, reported at the last meeting of COSPAR, by Austin, Purcell, Snider, Tousey, and Widing[1], were obtained with a single concave grating at normal incidence, and with an unbacked, 1000 Å thick, Al filter to eliminate long wavelength stray light. The images showed emission high in the corona in lines requiring coronal temperatures for their production. On April 28, 1966 coronal emission was observed to 5' above the limb, almost equally in Fe XV 284 Å, and Fe XVI 335, 361 Å, and decreasingly in the progression Fe XIV at least to Fe XII. Coronal emission was also associated with He II 303.8 Å, a chromospheric line; as suggested by Smith[2], this may be attributed to the near-blend, Si XI, 303.4 Å.

Since a large fraction of the spectral lines in the range 171 - 650 Å, covered by the spectroheliograph, are coronal and high chromospheric, it appeared possible that emission much higher than 5' above the limb might be detected if longer exposures, or an instrument having greater sensitivity were employed. For this purpose, an instrument which we call an XUV "heliograph" was devised. It is

---

*Supported, in part, by the National Aeronautics and Space Administration.

simply an XUV spectroheliograph without spectral dispersion . It utilized an off-axis, normal-incidence paraboloidal mirror of 50 cm or 25 cm focal length, and Schumann-type SC-7 film. The essential component is a series of aluminum filters. Each filter has maximum transmittance just longward of the $L_{2,3}$ edge at 171 Å, decreasing gradually to zero at $\lambda > 830$ Å. These filters are 1000 Å thick, and are mounted on 80 per inch Buckbee-Meers screens. With only a mirror, and no grating, it was necessary to use three of these filters in tandem to exclude all visible and near ultraviolet, because pinholes are almost always present to some extent in these thin films.

The efficiency of this instrument averaged 0.055 percent, and was moderately flat from 171 Å to 500 Å, because the spectral reflectance curve of the platinized mirror and the spectral transmittance curve of the Al filters compensated each other. To longer wavelengths the efficiency became very low. However, since the energy in the entire solar spectrum from 171 Å to about 500 Å is of the order of 2 ergs $cm^{-2} s^{-1}$, (Hinteregger[3]) and was concentrated in a single image, exposures were secured in as little as 2 sec.

The XUV heliograph was flown for the first time on July 27, 1966. Figure 1 shows 2 sec and 15 sec heliograms, compared with CaK and H-α spectroheliograms made on the same day at the McMath-Hulbert Observatory. The criss-cross structure in the heliograms is spurious, of course, and is associated with the screens on the filters were mounted. The difference between the XUV and the CaK and H-α images is striking. The emission from the plages is much more intense relative to the quiet disk in the XUV than in CaK, a narrow limb-brightened ring is present in the XUV, with maximum intensity in the equatorial regions; the limb brightening extends over the North Pole, but is conspicuously absent over the South. In places it is lost in stronger emission associated with centers of activity, extending into the corona. This was, of course, expected from the earlier XUV spectroheliograms which showed that the disk emission comes principally from lower-stage ions, such as He II 304 Å and the rest of the He II Lyman series. The narrow limb is caused partly by He II 304 Å, but to a greater extent by Ne VII 465 Å, Mg IX 369 Å, and the progression Fe VIII at least to XI, and perhaps to Fe XIV. The centers of activity are contributed to by all the lines, but especially by the very high-stage ions of Fe, Si and Mg.

Perhaps most striking is the intense coronal emission in the NW, of which there is no suggestion in CaK and H-α. In the NE there is even stronger and higher coronal emission; although much of this must come from the large places present in CaK, the intensity is so great that another source seems to be suggested. Inspection of the Fraunhofer Institut maps for adjacent days shows that there were intense centers of activity behind the limb on July 27; McMath plage 397 went over the west limb two days earlier, and plages 399 and 400 were just about on the limb on July 27. On the East, there was another intense plage, McMath 415, that was just in front of the limb, and can be seen in the CaK image. This, combined with a large plage well inside the limb, No. 414, must account for the corona, since on succeeding days no intense plages appeared in this region.

In Figure 2, 60-sec and 2-sec heliograms are shown, together with the 9.1 cm Stanford Radio Emission Spectroheliogram. It is evident that the 9.1 cm map agrees rather well with the short XUV picture; the coronal emission in the NW is present. Likewise the coronal emission in the NE is recorded with great intensity. The details of plages and the limb do not agree perfectly; the narrow limb-brightened ring is not clear in the radio map, nor is the weakening of the South Polar region.

The 60-sec exposure shows emission extending far beyond the limb, whose location is indicated by the circle (in preparing the reproduction, the image was cut off too close). In the SE the emission can be followed in the original to about 3 R_s, but in the NE and SW the edges of the film set the limit. Tests of the instrument after recovery ruled out the possibility that scattering effects caused any significant part of this emission. Therefore it is believed to be real XUV emission from the far-out corona.

A comparison was made between the 15-sec XUV corona exposure, the white-light corona as recorded by the K-coronameter of the High Altitude Observatory (Hanson[4]) and the intensity pattern of Fe XIV 5303 Å emission 1' above the limb. The result is shown in Figure 3. Here the K-coronameter data are plotted for a position 2' off the limb. Both intensity plots are radial, with the limb as origin. There is excellent qualitative agreement between all three patterns. Even details in the XUV corona are matched by the Fe XIV plot. This is not surprising, because the XUV range includes the Fe XIV resonance lines and others in the same high temperature range. The K-coronameter data show that the white-light corona also follows the XUV emission.

The extended XUV corona, unlike the white-light corona, cannot be attributed to Thompson scattering because its intensity is too great. Photometry of the XUV images gives intensity values at $R = 2 R_s$ that are 0.1 of the average intensity over the disk itself. But the white-light corona, even close to the limb, has an intensity not greater than 10^{-6} of the mean solar brightness, and Thompson scattering is independent of wavelength. Therefore the XUV corona must be caused by optical transitions in ions present in the corona. The intensity of this type of emission, if produced by collisional excitation, would be proportional to the electron density squared. It is surprising, therefore, that the intensity falls so much more slowly with R than does the white-light corona.

An alternative, and perhaps more reasonable explanation of the extended XUV corona is that it is associated with the high coronal abundance of Fe in the corona (Pottasch[5]), that seems to be required to explain the high intensity of the XUV emission lines of highly ionized Fe. According to Brandt[6], the reduced escape rate of Fe relative to H would cause a cloud of Fe to form around the sun. Contributing, might be an influx of meteoritic material. An enhanced concentration of Fe XIV, XV, XVI, together with radiative excitation of the XUV resonance lines would explain the principal characteristics of the XUV emission. Collisional excitation, ionization, and recombination would be expected to be present too. But the great intensity relative to the disk emission, decrease with R, and absence of any detail following streamers, indicates that optical excitation may dominate. This alone, without an increased Fe XIV - XVI density is not enough, because the XUV intensity should decrease with R like the K-corona, if Fe maintains its photospheric abundance relative to protons and electrons. The XUV coronal emission is strongest over centers of activity, but continues on out into the corona in a rather smooth fashion. Its distribution far out in the corona follows in a general way its emission distribution close in. The far-out emission shown by the 60-sec exposure is weakest over the poles, and strongest in the ENE and NW, following the emission close in shown by the short exposures. The emission far out in the SE does seem to be surprisingly intense, relative to the lower activity in southern latitudes, but this may be in part a photographic effect. However, in this and also in later flights the XUV does not show the irregular structures present in the K-corona from $R = 1$ to R_s; if present, they are too faint to detect. Radiative excitation, along with some collisional excitation, and a cloud of Fe ions seems to offer an explanation.

A more complete experiment was flown on November 12, 1966 to tie into the extensive observations to be made from the ground during the total solar eclipse. A pair of photographic white-light coronagraphs covering the region $R = 3$ to $9\ R_s$ was launched from the White Sands Missile Range in an Aerobee-150 rocket. Complete coverage in angle was obtained with the two instruments because the arms supporting the external occulters lay in opposite positions. The XUV heliograph was also flown, but with a 25 cm focal length paraboloid in order to provide wider angle coverage in the narrow direction of the photographic film.

The results of the November 12, 1966 experiment are shown in Figures 4 - 7. In Figure 4 a short-exposure XUV heliogram is introduced to scale at the center of the white light coronal eclipse photograph obtained by Newkirk during the High Altitude Observatory - The Johns Hopkins University Expedition to Bolivia. Below is a long-exposure XUV heliogram with the position of the photosphere drawn in. Close to the limb the white-light corona correlates very well with the XUV corona, just as was the case on July 27, 1966. Farther out the XUV camera becomes more uniform, and does not show the detail that is present in white light.

The NRL white-light corona is shown in Figure 5, pieced together from exposures made with the two instruments, thus eliminating the arms' shadows; a few artifacts were removed, but the dark ring and spiral at the South are instrumental. The moon is seen at the edge of the field, as described in the accompanying paper "The Moon Photographed at 2° Elongation" by M. J. Koomen, R. Tousey, and R. T. Seal, Jr.

In the center the corona photographed by Newkirk is introduced on the same scale. In both instruments an adjustment was made for the decrease of coronal brightness with increasing radius, therefore in each photograph the corona appears to be uniform, radially. Venus is present at about 4 R_s in the NE. At the very center, and blocking out the innermost portion of Newkirk's high-resolution coronal photograph, an XUV heliogram is introduced, as in Figure 4.

The corona recorded by Newkirk matches well the outer white-light corona photographed from the rocket. However, the great detail visible in most parts of the corona at $< 2 R_s$, is absent at $> 3 R_s$. Although this may, in part, be caused by the rotation of the field of the rocket coronagraph during the exposure, the reduced detail, far from the limb, appears to be real. There is only one strong streamer, and this reaches the edge of the field. On the original there is another streamer at about 40° W of N; this does not seem to be an extension of the fine, pointed streamer in Newkirk's photograph; it lies a bit to the West and is the extension of a diffuse, faint streamer in the eclipse photograph. The corona from $R = 3$ to $9 R_s$ follows the faint parts of the eclipse photograph at $R = 2$ to $3 R_s$, rather than the intense features closer in. The prominent streamer in the SW expands outward, and is straight. The regions over the poles are relatively dark; the seemingly greater intensity at large R over the South Pole than the North is probably an effect of printing.

In Figure 6 a long and a short XUV image are compared with the Stanford 9.1 cm Radio Emission Spectroheliogram for November 12, 1966. As on July 27, 1966, the correlation of details is good, but not exact. The XUV corona did not extend as far beyond the limb on November 12 as on July 27. The reason is not clear, and may be instrumental.

In Figure 7 a short-exposure XUV heliogram for November 12, 1966 is reproduced, together with a plot of Fe XIV 5303 Å intensities, recorded by the Sacramento Peak Observatory. Here, again, the correlation is good, as was the case on July 27, 1966. In reproduction the heliogram was improperly oriented by about 5°. Making an allowance for this, the details in the XUV corona above the limb match the Fe XIV data very well.

The white-light coronagraphs and the XUV heliograph were flown again on May 9, 1967 when the moon came close to the sun but did not produce a total eclipse. In Figure 8 a single coronal photograph is reproduced. This was prepared by splicing together the sections of the pair of photographs so as to eliminate the shadow of the arm. The moon is obvious; Mercury is the bright object at the very edge of the field exactly at the West. An XUV heliogram is introduced at the center of the shadow produced by the occulter.

In Figure 9 an XUV heliogram for May 9, 1967 is compared with a Ca-K spectroheliogram and the Fe XIV 5303 Å data from the Pic du Midi for the previous day. In Figure 10 a short and a long exposure XUV heliogram for this date are compared with the Stanford 9.1 cm map.

Although the provisional Zurich sunspot number was only 25 on May 9, 1967 compared with 80 on November 12, 1966 and 52 on July 27, 1966, it is obvious that there are many more plages, and that the Southern Solar Hemisphere had become more active with the increasing solar cycle. As usual, features show in the XUV that are not present in Ca-K; the agreement with the 9.1 cm map is much better than with Ca-K, but there are many differences in detail. This time, the long exposure shows strong emission over equatorial regions out to $3\ R_s$, as was the case on July 27, 1966. The emission over the North Pole remains more intense than over the South. No detailed structures are present in the far-out corona. Again, the 5303 Å distribution agrees very well with the XUV heliogram and both emissions extend over the South as well as the North Polar Regions.

Examining Figure 8 in detail, we see many streamers. To the East and West they are packed densely together. There is little North-South asymmetry. Two prominent streamers are present at high latitudes in the North, but there are none in the South.

The conspicuous characteristic of all the streamers is that they are straight. In the great groups to the East and West they are generally, but not exactly, radial. None of the streamers shows any appreciable garden-hose effect. The streamers just west of the North Pole are quite sharp and narrow, and nearly radial. We suppose that they originate from centers of activity on the rear side, at perhaps 45° Latitude, but at this time their points of origin have not been determined. It is possible that they are related to the coronal extensions shown in the 9.1 cm map; projecting them as straight lines does, indeed lead to the two 9.1 cm features near the North Pole.

The straightness of the streamers from $R = 3$ to $9\ R_s$ indicates that the solar wind in this region is no longer controlled by complex solar magnetic field; this is unlike the situation at $R = 1$ to 2 or 3, where eclipse photographs show clearly the connection between the field and the corona. Absence of the garden-hose effect leads to the conclusion that the flow of electrons out of the streamer is so rapid, relative to the sun's rotation, that the streamers appear to rotate rigidly out at least to 9 R_s.

REFERENCES

1. W. E. Austin, J. D. Purcell, C. B. Snider, R. Tousey, and K. G. Widing, Space Research VII, North-Holland Publishing Co. p. 1252, 1967.

2. T. S. Smith, discussion at the meeting of the American Astronomical Society, Boulder, Colorado, October 3, 1966.

3. H. E. Hinteregger, Space Science Rev. 4, 461, 1965.

4. R. T. Hansen, High Altitude Observatory, Mauna Loa, Hawaii, private communication.

5. S. F. Pottasch, Space Science Rev. 3, 816, 1964.

6. J. S. Brandt, Astrophysical J. 143, 265, 1966.

Figure Captions

Fig. 1. XUV heliograms, 2-sec and 15-sec exposure, compared with CaK and H-α spectroheliograms from the McMath-Hulbert Observatory July 27, 1966.

Fig. 2. The 60-sec and 2-sec XUV heliograms for July 27, 1966, compared with the 9.1 cm Stanford Radio Spectroheliogram, with contours, 4, 20, 25 and 62.5×10^{4} °K.

Fig. 3. The July 27, 1966 15-sec XUV heliograms, the K-coronameter 2' off-limb intensity recorded by the High Altitude Observatory, and the coronal green line intensity from Norikura.

Fig. 4. The white-light corona during the November 12, 1966 eclipse (Newkirk, HAO) and the NRL XUV corona. A short exposure is introduced, to scale, at the center of the eclipse photograph; exposure is shown below, with the position of the photosphere sketched in.

Fig. 5. The sun on November 12, 1966:
The outer white-light corona, NRL Rocket Coronagraph;
the inner white-light corona, HAO;
an XUV image of the sun, NRL Heliograph.

Fig. 6. Short and long exposure. XUV heliograms for 12 November 1966, compared with the Stanford 9.1 cm Radio Emission Spectroheliogram. The contours are 4, 10, 25 and 62.5 x 10^4 °K.

Fig. 7. An XUV heliogram compared with the Fe XIV 5303 Å intensity from Sacramento Peak, November 12, 1966 (the rotational position of the heliogram is incorrectly registered by about 5°).

Fig. 8. The white light corona on May 9, 1967; this is a composite of a pair of exposures made with the two instruments. The XUV heliograms is introduced at the position of the sun, and to scale.

Fig. 9. An XUV heliogram and a Ca-K spectroheliogram for May 9, 1967. The Fe XIV 5303 Å distribution is from the Pic du Midi for May 8.

Fig. 10. Short and long exposure. XUV heliograms for May 9, 1967 and the Stanford 9.1 cm Radio Emission Spectroheliogram.

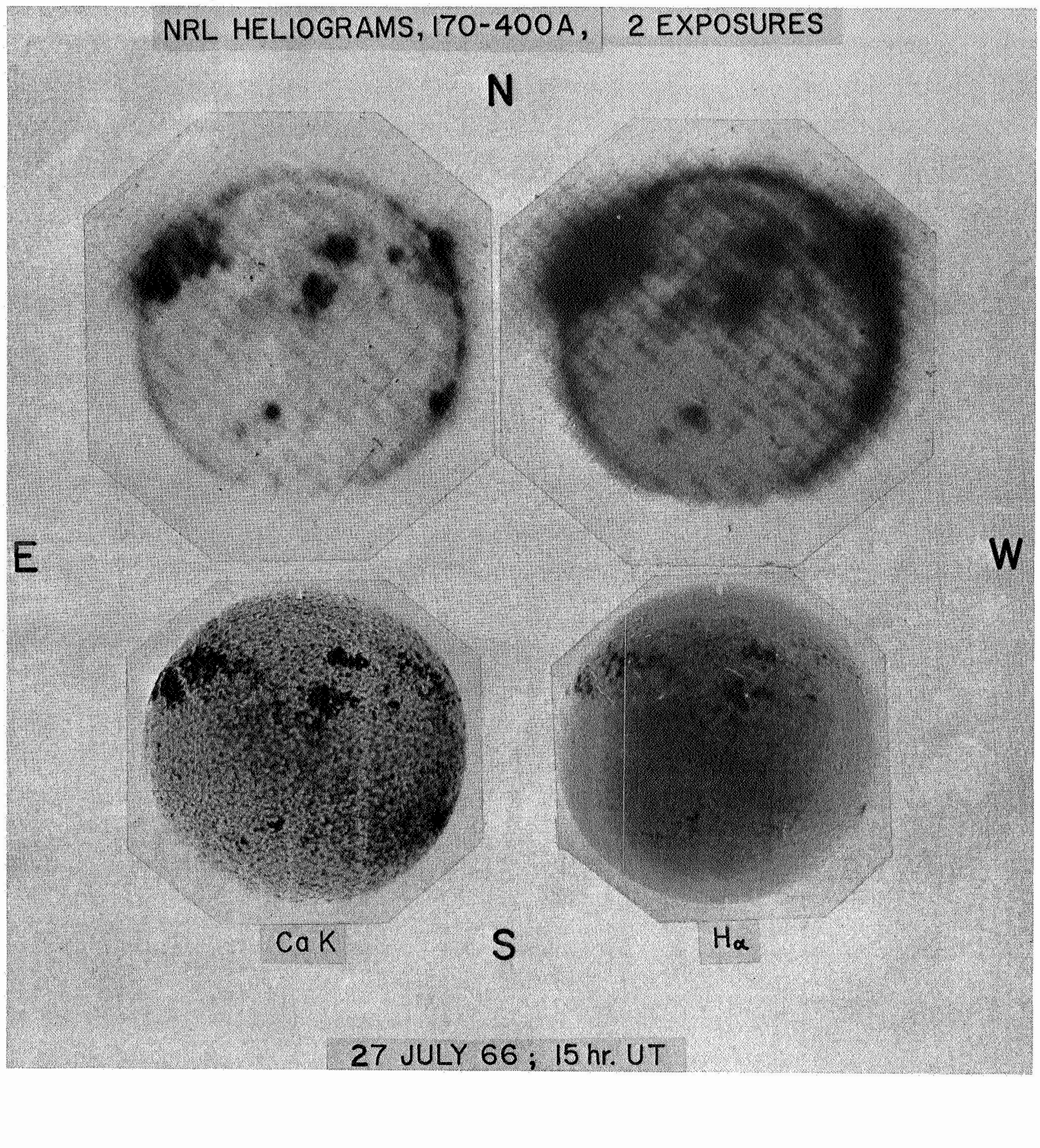
NRL HELIOGRAMS, 170-400A, 2 EXPOSURES
N
E
W
Ca K
S
Hα
27 JULY 66 ; 15 hr. UT

Figure 1

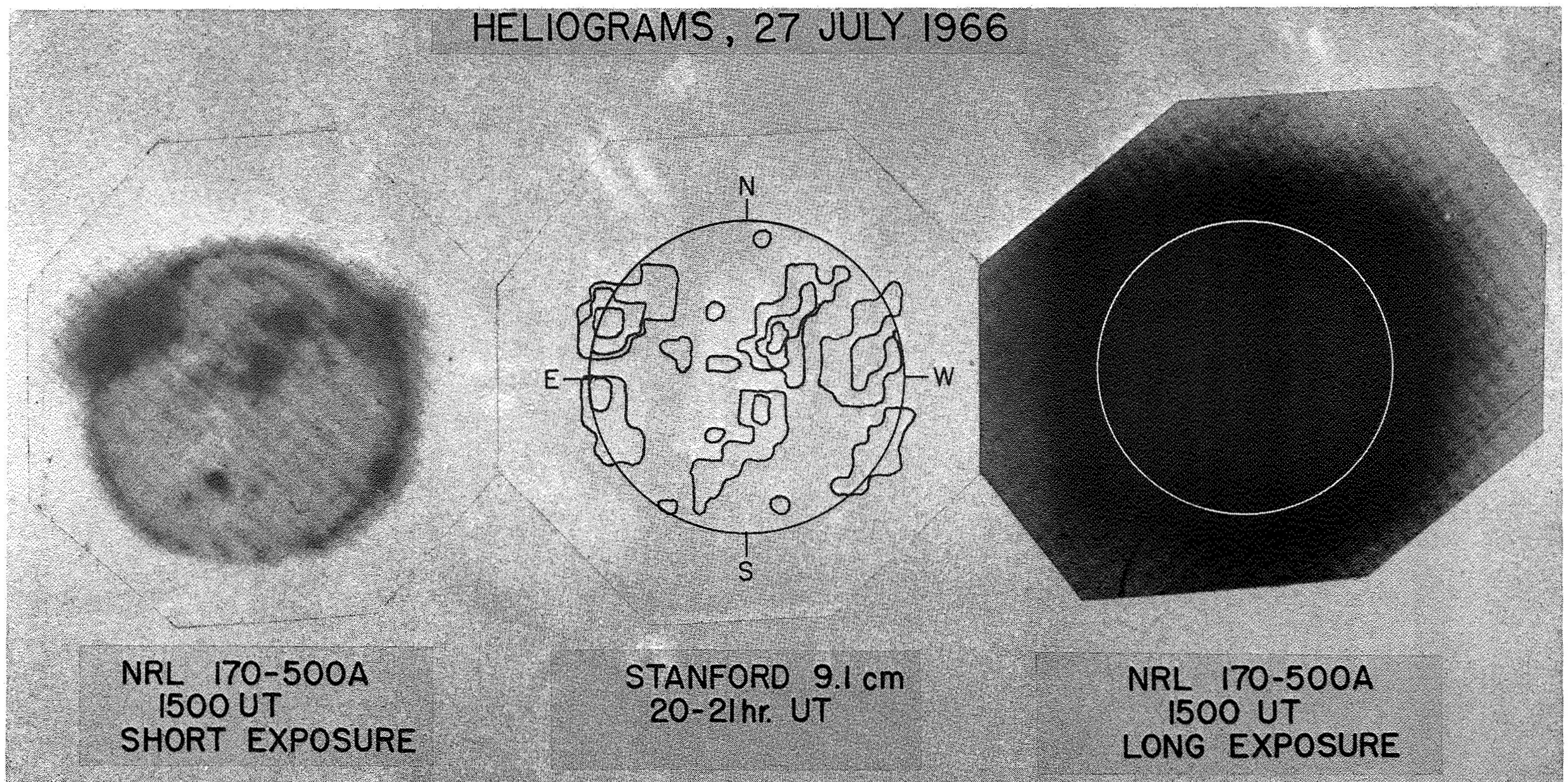
HELIOGRAMS, 27 JULY 1966
N
E
W
S
NRL 170-500A
1500 UT
SHORT EXPOSURE
STANFORD 9.1 cm
20-21hr. UT
NRL 170-500A
1500 UT
LONG EXPOSURE

Figure 2

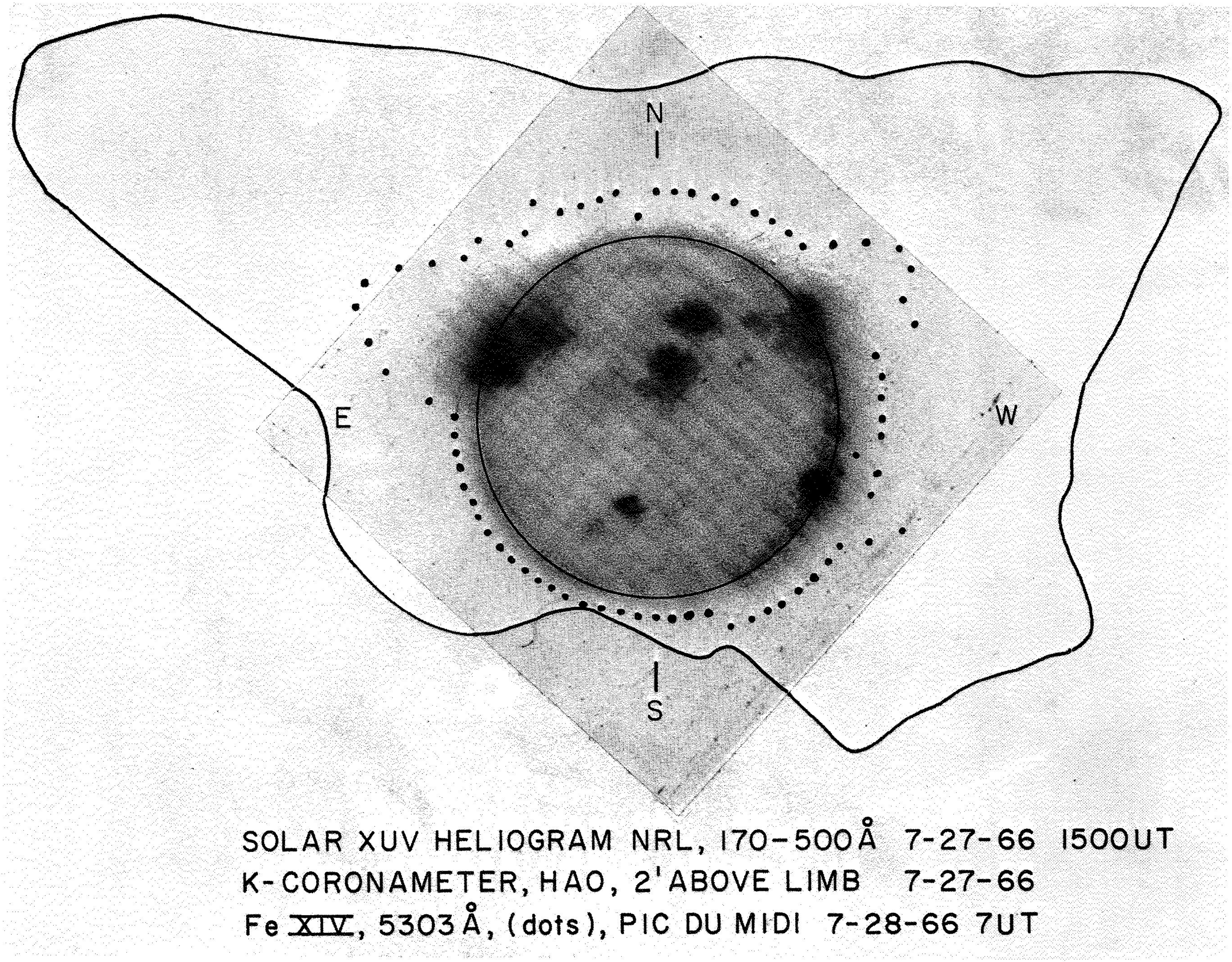
N
E
W
S
SOLAR XUV HELIOGRAM NRL, 170-500 Å 7-27-66 1500 UT
K-CORONAMETER, HAO, 2' ABOVE LIMB 7-27-66
Fe XIV, 5303 Å, (dots), PIC DU MIDI 7-28-66 7UT

Figure 3

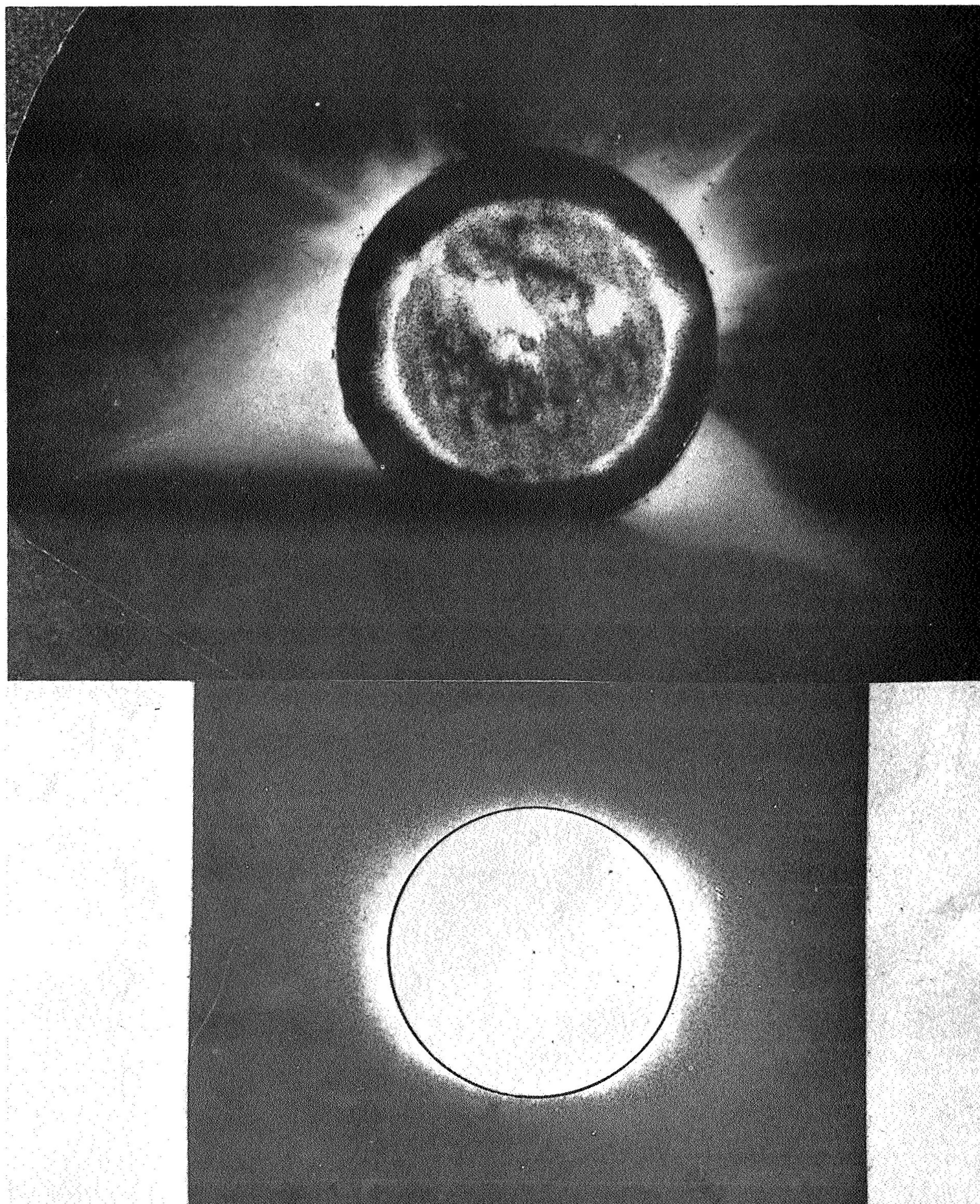

12 NOV. 66 1620 UT

TOP: CENTER, XUV SOLAR DISK 170 - 400 Å NRL

OUTSIDE, WHITE-LIGHT CORONA NEWKIRK HAO

BOTTOM: XUV SOLAR DISK 170 - 400 Å LONG EXPOSURE NRL

Figure 4

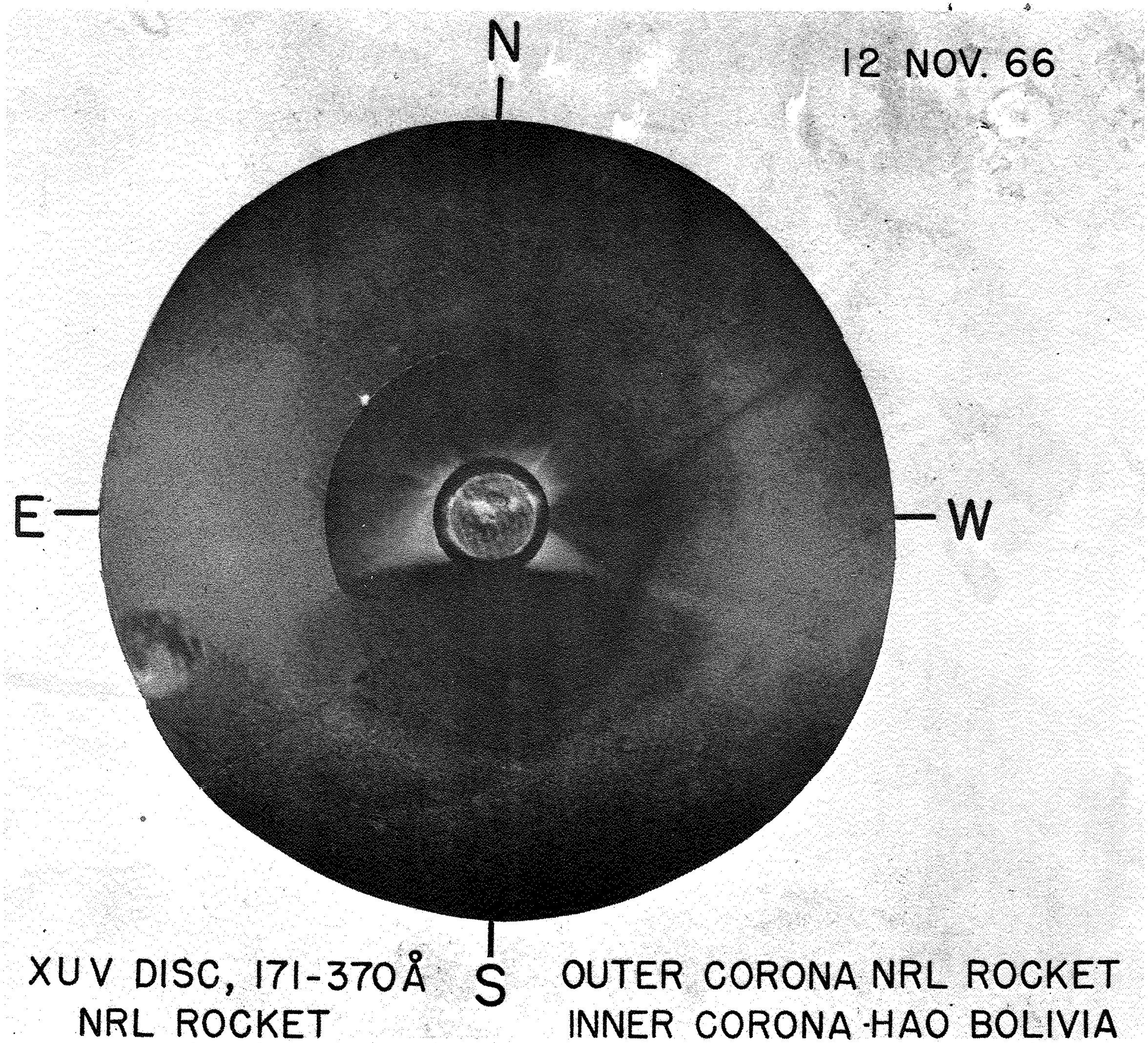
N
12 NOV. 66
E
W
S
XUV DISC, 171-370Å
NRL ROCKET
OUTER CORONA NRL ROCKET
INNER CORONA-HAO BOLIVIA

Figure 5

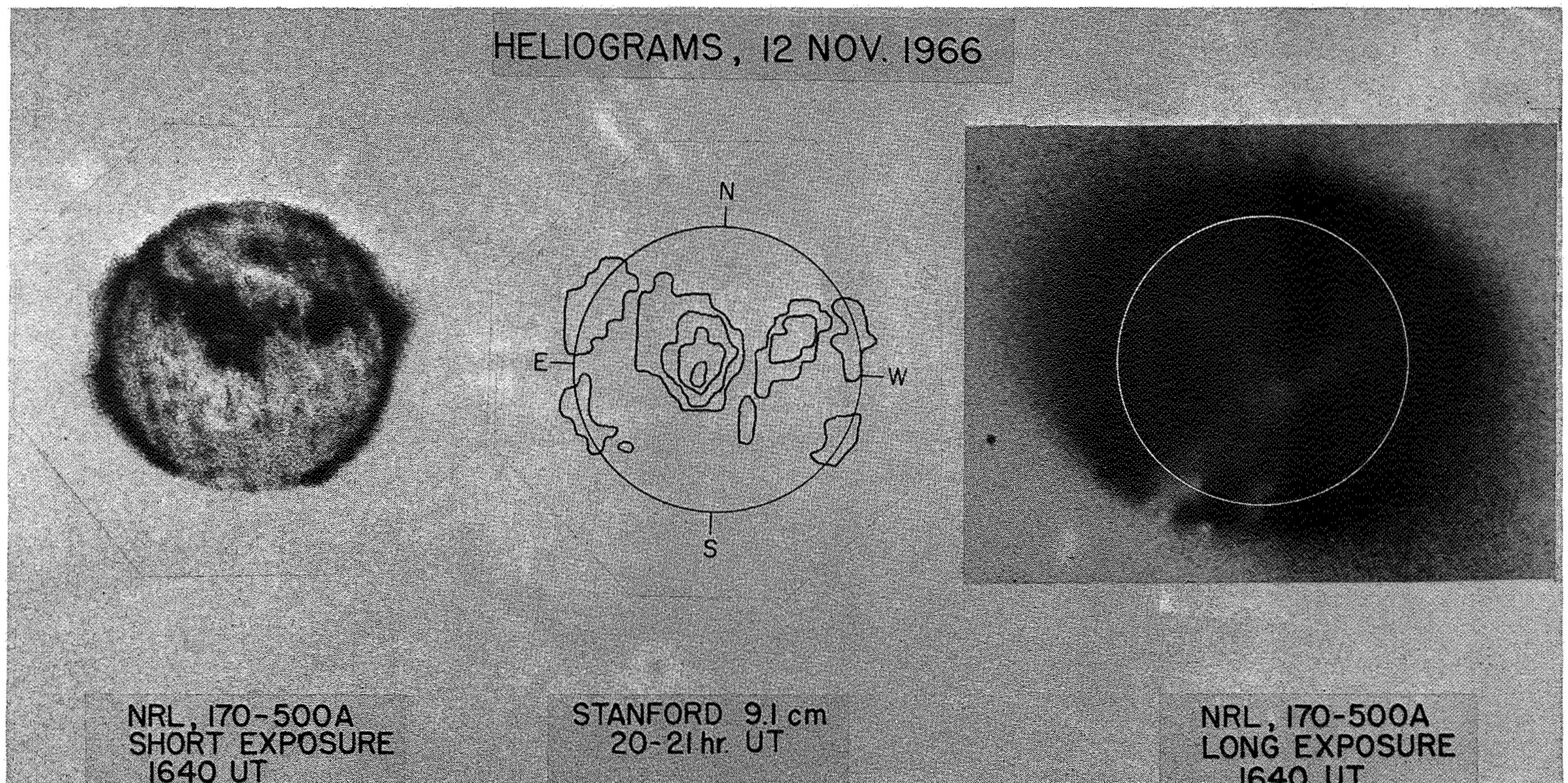
HELIOGRAMS, 12 NOV. 1966
N
E
W
S
NRL, 170-500A
SHORT EXPOSURE
1640 UT
STANFORD 9.1 cm
20-21 hr. UT
NRL, 170-500A
LONG EXPOSURE
1640 UT

Figure 6

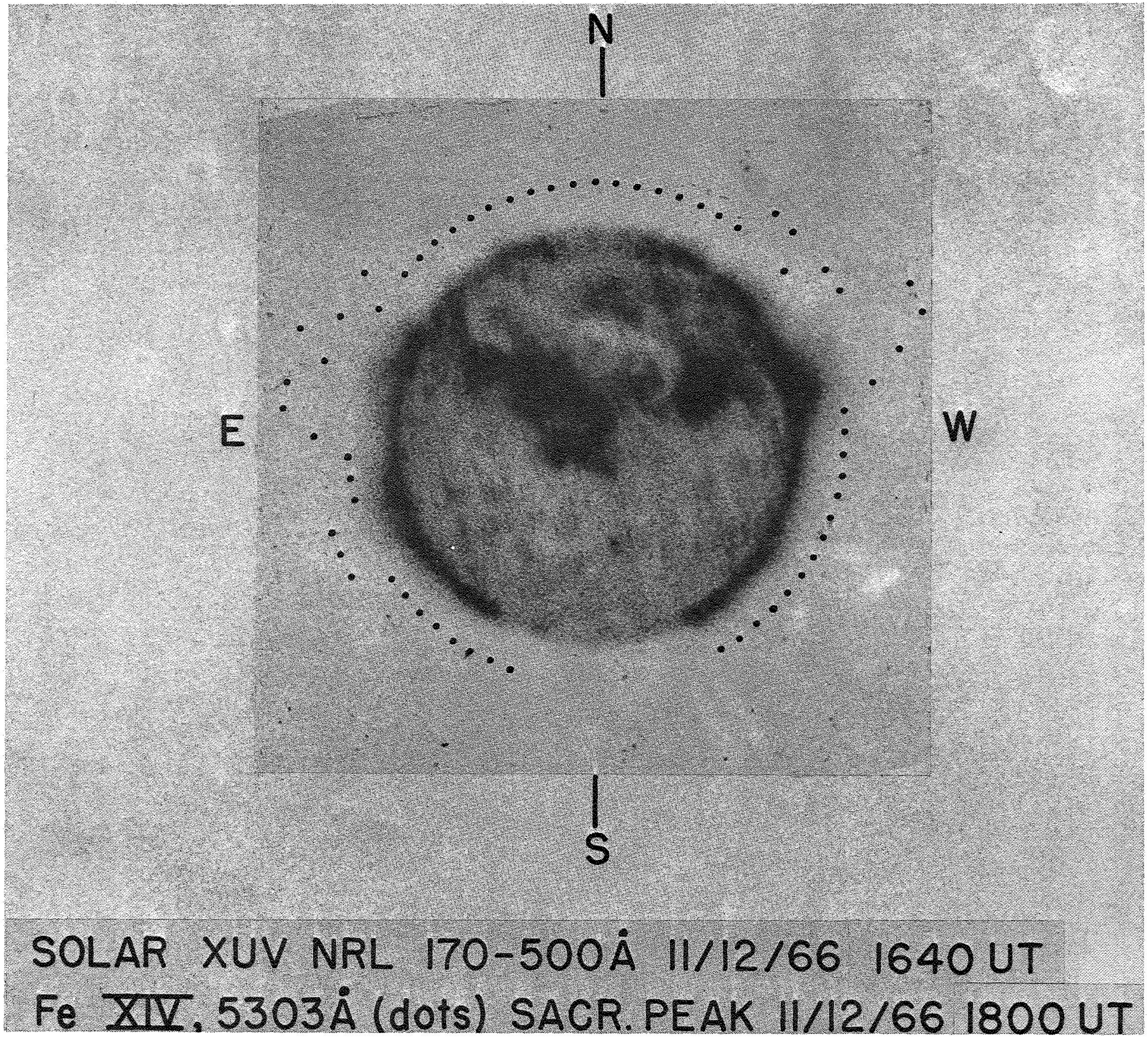
N
E
W
S
SOLAR XUV NRL 170-500Å 11/12/66 1640 UT
Fe XIV, 5303Å (dots) SACR. PEAK 11/12/66 1800 UT

Figure 7

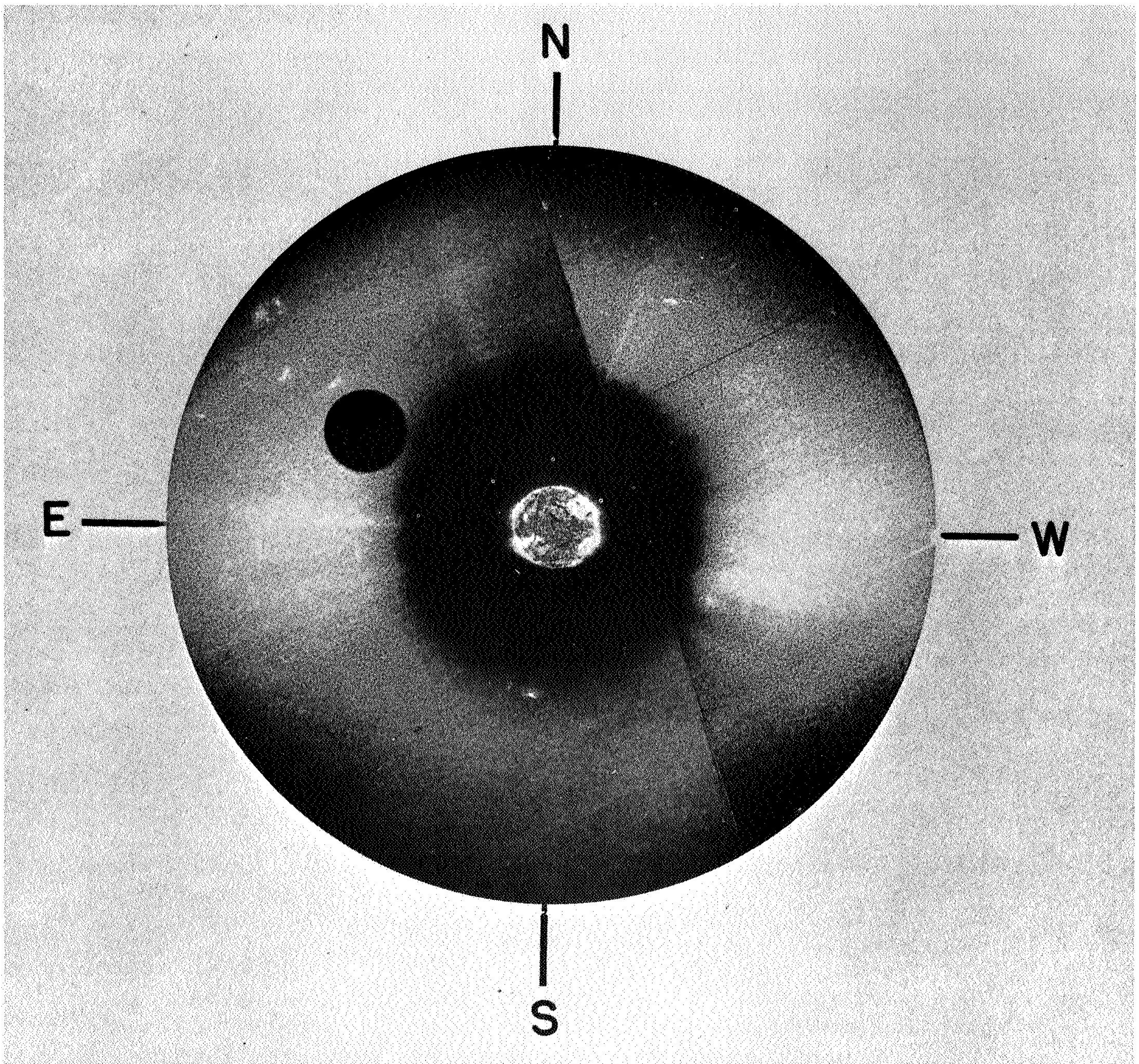

COMPOSITE, CORONAGRAPH FRAMES 53A & 53B
AND XUV SUN (171-370 A)
WSMR 9 MAY 1967 1618 UT

Figure 8

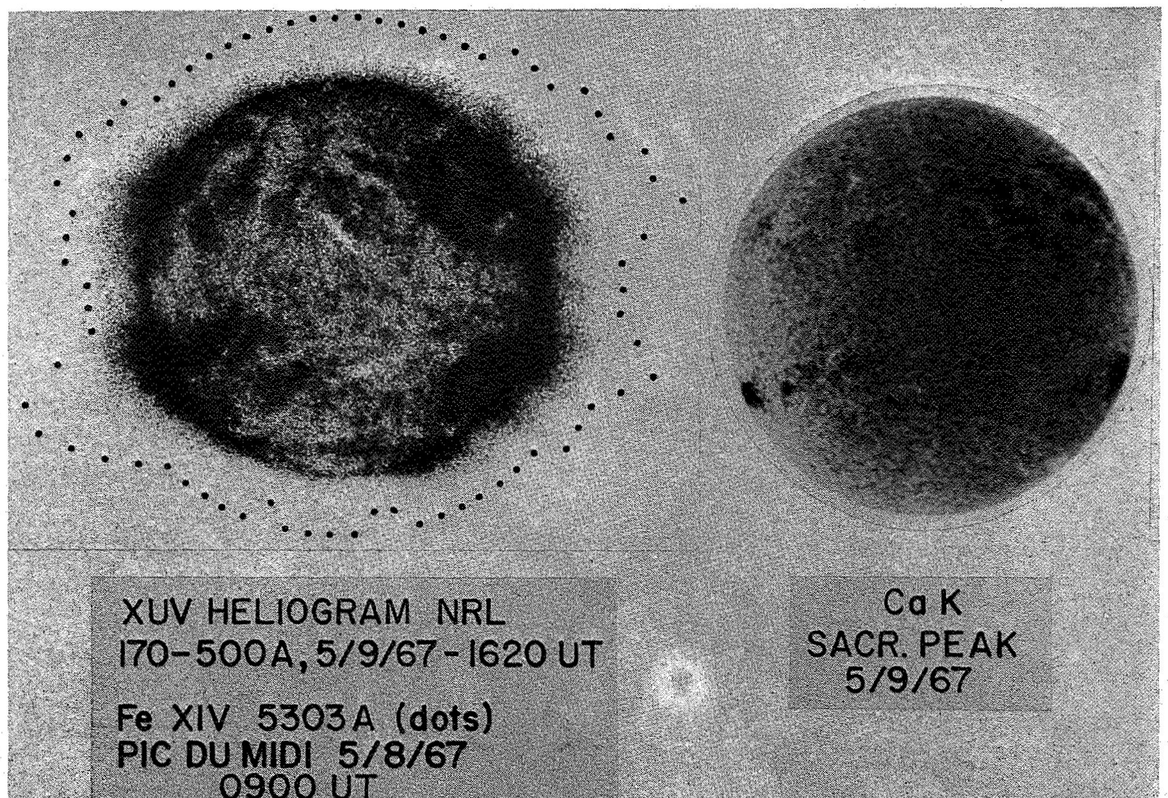
XUV HELIOGRAM NRL
170-500A, 5/9/67-1620 UT
Fe XIV 5303A (dots)
PIC DU MIDI 5/8/67
0900 UT
Ca K
SACR. PEAK
5/9/67

Figure 9

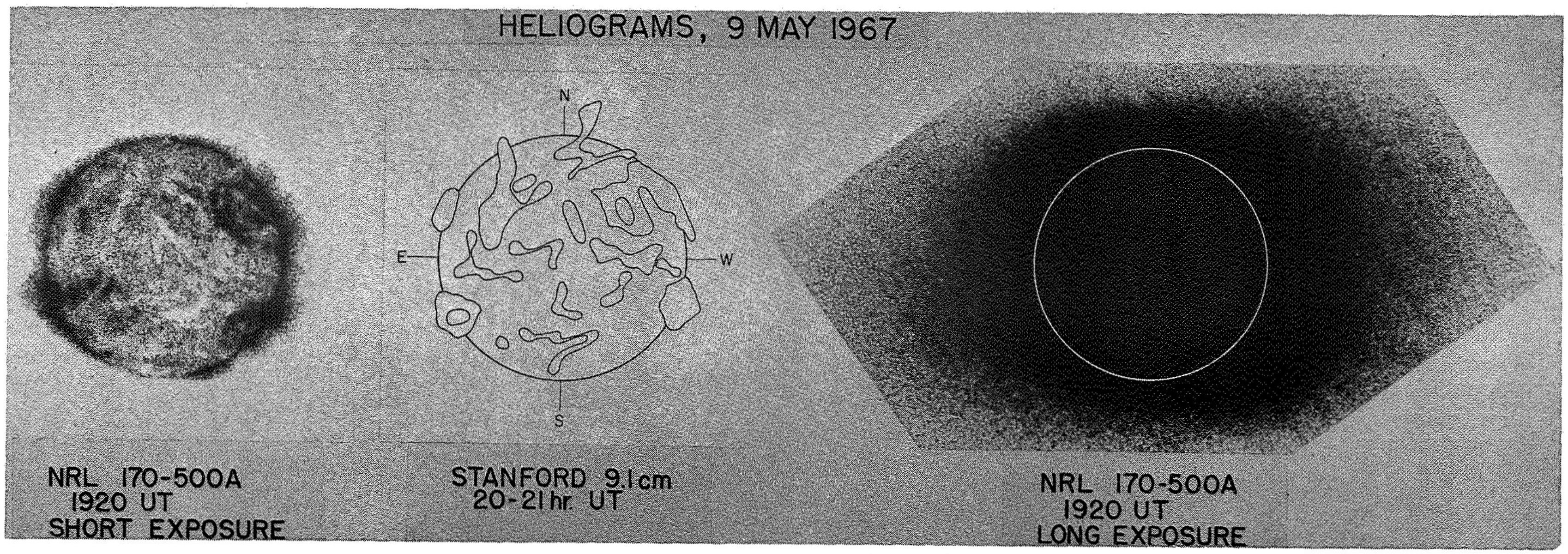

HELIOGRAMS, 9 MAY 1967
N
E
W
S
NRL 170-500A
1920 UT
SHORT EXPOSURE
STANFORD 9.1cm
20-21hr. UT
NRL 170-500A
1920 UT
LONG EXPOSURE

Figure 10